Determination of Phase Behavior of Poly(ethylene oxide) and Chitosan Solution Blends Using Rheometry

ARTICLE *in* MACROMOLECULES · SEPTEMBER 2012

Impact Factor: 5.8 · DOI: 10.1021/ma301193h

3 AUTHORS, INCLUDING:

Mehdi Pakravan
Polytechnique Montréal
5 PUBLICATIONS **99** CITATIONS

Macromolecules

Article

pubs.acs.org/Macromolecules

Determination of Phase Behavior of Poly(ethylene oxide) and Chitosan Solution Blends Using Rheometry

Mehdi Pakravan, Marie-Claude Heuzey,* and Abdellah Ajji*

CREPEC, Department of Chemical Engineering, Ecole Polytechnique de Montreal, P.O. Box 6079, Station Centre-Ville, Montreal, Quebec, Canada H3C 3A7

ABSTRACT: Aqueous solutions of PEO exhibit a lower critical solution temperature (LCST) phase diagram. In this work, phase separation behavior of PEO/water solutions was investigated using small-amplitude oscillatory shear and steady shear rheological measurements. Binodal decomposition temperatures were determined from the sudden changes in the slope of the dynamic temperature sweep of storage modulus and loss tangent. The spinodal decomposition points were also estimated by a mean-field theoretical approach. Comparing the obtained critical points with other conventional methods revealed that rheological measurements are powerful and sensitive to detect even the early stage of phase separation of PEO solutions. This successful method was employed to investigate phase separation and miscibility of chitosan/PEO solutions at different compositions in aqueous acetic acid solutions that have already showed anomalous behavior in a forming process. Lower critical solution temperature (LCST) phase behavior was observed for chitosan/PEO solution blends. Phase separation temperature, miscibility range, and correlation length of the solutions were determined from isochronal dynamic temperature sweep experiments. The effect of chitosan/PEO ratio on the binodal and spinodal decomposition temperatures was studied. Finding phase separation information on polymer solutions through rheological measurement is very promising. Isothermal steady shear rheological measurements were also carried out on chitosan/PEO solutions over a temperature range in which phase separation occurs. Viscosity increase at low shear rates above but in the vicinity of phase separation temperature was observed, which confirms the validity of the theoretical approach employed to determine the critical temperatures through dynamic rheological measurements. Finally, the Flory–Huggins interaction parameters were estimated from critical solution temperature and concentration results.

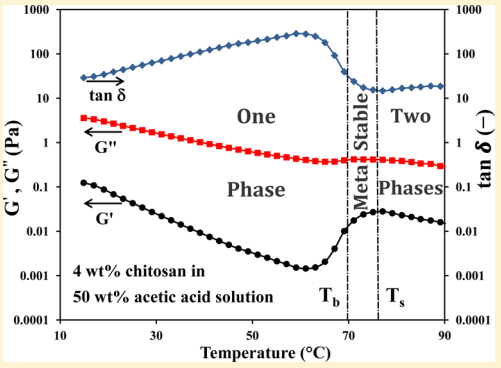

1. INTRODUCTION

PEO is a water-soluble, hydrophilic, nontoxic, and biocompatible polymer that has been widely used for biomedical and biomimetics applications.[1−3] Phase separation behavior and solubility characteristics of aqueous solutions of poly(ethylene oxide) (PEO) have been raising both scientific and industrial interests for more than four decades.[1,3−9] Aqueous PEO solutions exhibit anomalous behavior in contrast to other ordinary polymer solutions. They show an inverse solubility−temperature relationship that leads to a phase separation upon heating. At even higher temperatures the homogeneous state becomes stable again. Hence, a closed loop phase diagram is observed as one of the characteristic features of aqueous PEO solutions. However, for high molecular weight PEO grades, i.e., more than 100 kDa, only a low critical solution temperature (LCST) that depends on the molecular weight is observed.[4,6,9] Such extraordinary properties are seen only in highly polar systems that exhibit strong orientation dependence of molecular interactions such as hydrogen bonding.[1,4−6,10] Clustering (also referred to as aggregation) is another unusual characteristic of PEO solutions dissolved in water (or other solvents) that has been studied intensively by several authors.[2,3,5,7,9] Clusters or aggregates form in concentrated aqueous PEO solutions associated with temperature increase (T > 30 °C). The clustering effect is pervasive and has been observed in some other systems such as polyelectrolyte solutions and clay dispersions.[7,11,12] The basic origin of this cluster formation is not understood and remains an open question.[7,13] The peculiar behavior of aqueous PEO solutions is attributed to the existence of hydrogen bonds between ether groups in PEO and hydrogen in water molecule and how these bonds are affected by temperature.[1,3,7,8]

Chitosan is a linear polysaccharide that is mainly produced from the partial deactetylation of chitin, one of the most abundant polysaccharides in nature.[14−18] Chitosan is the only pseudonatural cationic polyelectrolyte. Aqueous acidic solutions of chitosan exhibit great solubility, similarly to aqueous PEO solutions, due to the presence of strong hydrogen bonds between the solvent and the polymer owing to the presence of hydroxyl, acetylamine, and amino groups on the chitosan chain. Therefore, the occurrence of an LCST in chitosan solutions is expected.[1,6] The tendency of chitosan to form aggregates in solution, which is attributed to the hydrophobic interactions of

Received: June 12, 2012
Revised: August 2, 2012
Published: September 11, 2012

residual acetylated groups,[16] has also been investigated extensively.[11,12,19]

Chitosan solutions and their blends with other synthetic polymers have recently attracted great attention[15,20−22] due to the following facts:

The fascinating features of chitosan including renewability, availability in nature, nontoxicity, biocompatibility, antibacterial, and biodegradability,[14,17,18] which makes it a promising choice for biomedical and pharmaceutical applications such as drug delivery systems, wound healing dressings, tissue engineering scaffolds, and antibacterial membranes.[18,21,23]

The "wet route" is the only successful method to fabricate chitosan final products in different forms of films, porous membranes, fibers, particles, or sponges.[15,21−24] Chitosan should be processed in a solution state for all final applications. "Dry methods" such as melt processing, plasticization, and kneading are still in early stages of research.[25−27]

Blending of chitosan in the solution state with other hydrophilic polymers such as PEO,[28−31] poly(vinyl alcohol) (PVA),[32,33] poly(acetic acid) (PLA),[25] and polycaproloctone (PCL)[34,35] is a well-known approach to facilitate its processing, improve final properties, or overcome the disadvantage of the loss in mechanical strength in the wet state.[29,36]

PEO is a more attractive polymer for blending with chitosan due to its solubility in various aqueous solvents and biocompatibility.[30] Consequently, understanding the phase behavior and miscibility of aqueous acidic solutions of chitosan and PEO and their blends is of crucial importance, as any phase separation occurring during the forming processes such as film casting, fiber spinning, and solution electrospraying greatly changes the morphology and physicomechanical properties of the final products.

In a separate study, the present authors have described an incoherent behavior of chitosan/PEO solutions in the electrospinning process at high temperatures.[29] We found that moderate process temperatures help to stabilize the electrospinning process of chitosan/PEO blend solutions and produce bead-less nanofibers. However, at higher temperature, the electrospun jet became unstable and beaded fibers morphology were obtained.[29] The relevance of this observation to the temperature-induced phase separation of these solutions was questioned. On the other hand, results of transmission FTIR on cast films and nanofibers of chitosan/PEO blends at room temperature showed the existence of hydrogen-bonding interactions between chitosan and PEO, an indication of miscibility of these two polymers.[29]

Several methods have been used to study the onset of phase separation in polymer systems. Simple visual observation of turbidity,[37,38] thermo-optical analysis (TOA),[6] light scattering,[3,5,39,40] and small-angle neutron scattering (SANS)[7,13] are frequently used to determine the early stages of liquid−liquid phase separation in polymer solutions. However, only improved scattering techniques yield more detailed information leading to both spinodal and binodal points (cloud points).[6,39,40] While the extensive studies were done to estimate the binodal (cloud points) temperatures, little work on spinodal point measurements of well-known PEO/water solutions have been published. The fact is that by having binodal and spinodal points one can calculate the values of Flory−Huggins interaction parameter (χ), a fundamental characteristic of polymer solutions.[10,41,42]

Rheometry represents a powerful tool to study the phase behavior of polymeric systems. Rheological measurements are sensitive to polymer chain reptation, diffusion, and interfacial tension and thus can be used to detect phase separation in rather early stages. Concentration fluctuations involving various mechanisms such as nucleation, diffusion, domain growth, and coagulation are generally considered as the physical source of phase separation.[43,44] Near the phase separation temperature, the linear viscoelastic response is influenced by the critical concentration fluctuations and exhibits a thermorheological complexity, i.e., enhancement of elasticity in the vicinity of phase separation.[44−47] Ajji and Choplin[48] quantified this phenomenon for polymer blends by extending the mean-field theories of Fredrickson and Larson[49] developed for copolymers. It was shown that this approach can determine both the spinodal[44−47] and binodal[44,45,50] temperatures by carrying out a dynamic temperature sweep test on the blend and tracking the evolution of rheological material functions G' and G''. This method was successfully employed for different polymer pairs, and the obtained data agreed well with that from other techniques such as optical microscopy,[47,51,52] light scattering,[46] and inverse gas chromatography.[43] Additionally, this quantitative technique allowed obtaining suitable results for both LCST[43,45,47,50,53] and UCST[44,46] systems.

In this paper we demonstrate the usefulness of the rheological approach to investigate the phase behavior of polymer solutions. To the best of our knowledge, it is the first time that this method is employed to study the liquid−liquid phase separation of a polymer solution. A PEO aqueous solution is selected as a model system to develop the experimental protocol, and subsequently the method is applied to aqueous acetic acid solutions of PEO, chitosan, and their blends at different ratios. The results are expected to provide a clear understanding about the phase behavior and miscibility of these blends, which is valuable for polymer forming processes in the solution state such as fiber spinning and film casting. Additionally, key macromolecular and thermodynamic parameters such as correlation length and Flory−Huggins interaction parameter (χ) of the polymer solutions are estimated from isochronal dynamic temperature sweep experiments.

2. THEORETICAL BACKGROUND

2.1. Scaling Analysis of Dynamic Rheological Properties near Phase Separation. Observations of anomalous behavior in dynamic rheological properties of block copolymer melts in the transitional regime of phase separation have been analyzed by Fredrickson and Larson.[49] They used a mean-field theory to derive the critical contribution of the concentration fluctuations to the viscoelastic properties of block copolymers near the critical point. After wave-vector integration, they obtained the following expressions for the dynamic storage (G') and loss moduli (G''):

$$G'(\omega) = \frac{k_B T \omega^2}{15\pi^2} \int_0^{k_0} \frac{k^6 {S_0}^2(k)}{\omega^2 + 4\bar{\omega}^2(k)} \left[\frac{\partial {S_0}^{-1}(k)}{\partial k^2}\right]^2 dk \quad (1)$$

$$G''(\omega) = \frac{2k_B T \omega}{15\pi^2} \int_0^{k_0} \frac{k^6 {S_0}^2(k)\bar{\omega}(k)}{\omega^2 + 4\bar{\omega}^2(k)} \left[\frac{\partial {S_0}^{-1}(k)}{\partial k^2}\right]^2 dk \quad (2)$$

where $\bar{\omega}(k) = k^2 {S_0}^{-1}(k)\lambda(k)$, $S_0(k)$ is a static structure factor, $\lambda(k)$ is the Onsager coefficient for the polymeric system of interest, k defines the wave vector, ω is the angular frequency, and k_B is the Boltzman coefficient. These equations are valid for both block copolymers and homopolymer blends. Hence, G'

and G'' can be calculated by using the appropriate expression of the static structure factor and the Onsager coefficient. Ajji and Choplin[48] extended Fredrickson and Larson's approach[49] to binary homopolymer blends after observing a similar behavior[52,54] in the evolution of their viscoelastic properties under oscillatory shear flow. They derived the previous equations (eqs 1 and 2) for homopolymer blends by using (1) the static structure factor computed by de Gennes by a mean-field approach in the random phase approximation

$$\frac{1}{S_0(k)} = \frac{1}{\phi N_1 g_1(k)} + \frac{1}{(1-\phi)N_2 g_2(k)} - 2\chi \tag{3}$$

where ϕ is the volume fraction of polymer 1, N_i is the number of statistical segments, and $g_i(k)$ is the Debye function and (2) the expression for the Onsager coefficient, $\lambda(k)$, proposed by Binder[48]

$$\frac{1}{\lambda(k)} = \frac{1}{\phi a_1^2 W_1 g_1(k)} + \frac{1}{(1-\phi)a_2^2 W_2 g_2(k)} \tag{4}$$

where a_i is the statistical segment length of the species i and W_i is its rate of orientation defined by

$$W_i = 3\pi k_B T/\zeta_i \tag{5}$$

where ζ_i is the monomeric friction coefficient.

Using eqs 3−5, Ajji and Choplin[48] integrated eqs 1 and 2 by considering an expansion of the Debye function in the homogeneous region near the critical point. More details of their development and discussion in the case of homopolymer blends can be found in ref 48. Finally the following expressions for G' and G'' were derived in the terminal one-phase region near the critical point:

$$G'(\omega) = \frac{k_B T \omega^2}{1920\pi}\frac{1}{3}\left\{\frac{R_{g_1}^2}{\phi N_1} + \frac{R_{g_2}^2}{(1-\phi)N_2}\right\}^{1/2} \left[\frac{1}{\phi a_1^2 W_1} + \frac{1}{(1-\phi)a_2^2 W_2}\right]^2 [2(\chi_s - \chi)]^{-5/2} \tag{6}$$

$$G''(\omega) = \frac{k_B T \omega}{240\pi}\frac{1}{3}\left\{\frac{R_{g_1}^2}{\phi N_1} + \frac{R_{g_2}^2}{(1-\phi)N_2}\right\}^{-1/2} \left[\frac{1}{\phi a_1^2 W_1} + \frac{1}{(1-\phi)a_2^2 W_2}\right] [2(\chi_s - \chi)]^{-1/2} \tag{7}$$

where χ_s is the value of the interaction parameter at the spinodal temperature, χ is the interaction parameter at temperature T, and R_{g_i} is the radius of gyration defined as $R_{g_i}^2 = N_i a_i^2/6$.

Using eqs 6 and 7, the ratio of $G'(\omega)/G''^2(\omega)$ can be calculated as follows, where the monomeric friction coefficient (ζ) is eliminated and there is no explicit dependency on angular frequency (ω):

$$\frac{G'}{G''^2} = \frac{30\pi}{k_B T}\left\{\frac{a_1^2}{36\phi} + \frac{a_2^2}{36(1-\phi)}\right\}^{3/2} (\chi_s - \chi)^{-3/2} \tag{8}$$

This expression is only valid for the terminal response (near the critical region), where G' and G'' have the scaling behavior of $G' \sim \omega^2$ and $G'' \sim \omega^1$, respectively. The expression for the correlation length of a binary polymer blend is

$$\xi = \frac{a'}{6}[\phi(1-\phi)(\chi_s - \chi)]^{-1/2} \tag{9}$$

where a' is the characteristic length which is defined based on the individual segment lengths in each phase, a_1 and a_2, using the equation

$$\frac{a'^2}{\phi(1-\phi)} = \frac{a_1^2}{\phi} + \frac{a_2^2}{1-\phi} \tag{10}$$

Thus, the correlation length can be calculated near the critical point directly from the shear rheological data:

$$\xi = \left[\frac{k_B T}{30\pi}\frac{G'}{G''^2}\right]^{1/3} \tag{11}$$

Assuming the following expression for the interaction parameter[55]

$$\chi = A + B/T \tag{12}$$

By substituting the interaction parameter in eq 8, one can find the following expression:

$$\left(\frac{G''^2}{TG'}\right)^{2/3} = \frac{B}{C}\left(\frac{1}{T_s} - \frac{1}{T}\right) \tag{13}$$

where C is given by

$$C = \left(\frac{5\pi}{36k_\beta}\right)^{2/3}\left[\frac{a_1^2}{\phi} + \frac{a_2^2}{1-\phi}\right] \tag{14}$$

Hence, a linear dependence of $(G'^2/G'T)^{2/3}$ versus $1/T$ is predicted for the blends at the phase transitional region. The spinodal decomposition temperature (T_s) is then calculated from the intercept of the line with the $1/T$ axis.

2.2. Evaluation of Flory−Huggins Interaction Parameter for Polymer Solutions from Their Critical Temperature and Concentration Data. In general, the Flory−Huggins expression for the molar Gibbs free energy of mixing of a binary polymer solution at temperature T is given by[42]

$$\frac{\Delta G}{RT} = \frac{\phi_1 \ln \phi_1}{r_1} + \frac{\phi_2 \ln \phi_2}{r_2} + \chi\phi_1\phi_2 \tag{15}$$

where ΔG is the free energy of mixing per unit volume, R is the universal gas constant, T is the absolute temperature, ϕ_1 and ϕ_2 and r_1 and r_2 are the volume fractions and relative molar volumes of component 1 and 2, respectively; $r_1 = 1$ for the solvent, and χ is the Flory−Huggins interaction parameter.

However, it has been shown in several works that χ depends on both temperature and polymer concentration.[41,56] Hence, in eq 15, a more general interaction function, $g(T,\phi_2)$, is suggested as a semiempirical form of χ. After replacing χ with $g(T,\phi_2)$, the Gibbs free energy function is written as eq 16 for describing the free energy of real systems:[10,56,57]

$$\frac{\Delta G}{RT} = \frac{\phi_1 \ln \phi_1}{r_1} + \frac{\phi_2 \ln \phi_2}{r_2} + g(T, \phi_2)\phi_1\phi_2 \tag{16}$$

Different functions have been proposed for the dependency of $g(T,\phi_2)$ on temperature and concentration.[37,41] It is shown that similar to several other polymer/solvent systems, for highly diluted PEO/water solutions interaction parameter χ starts out

dx.doi.org/10.1021/ma301193h | Macromolecules 2012, 45, 7621−7633

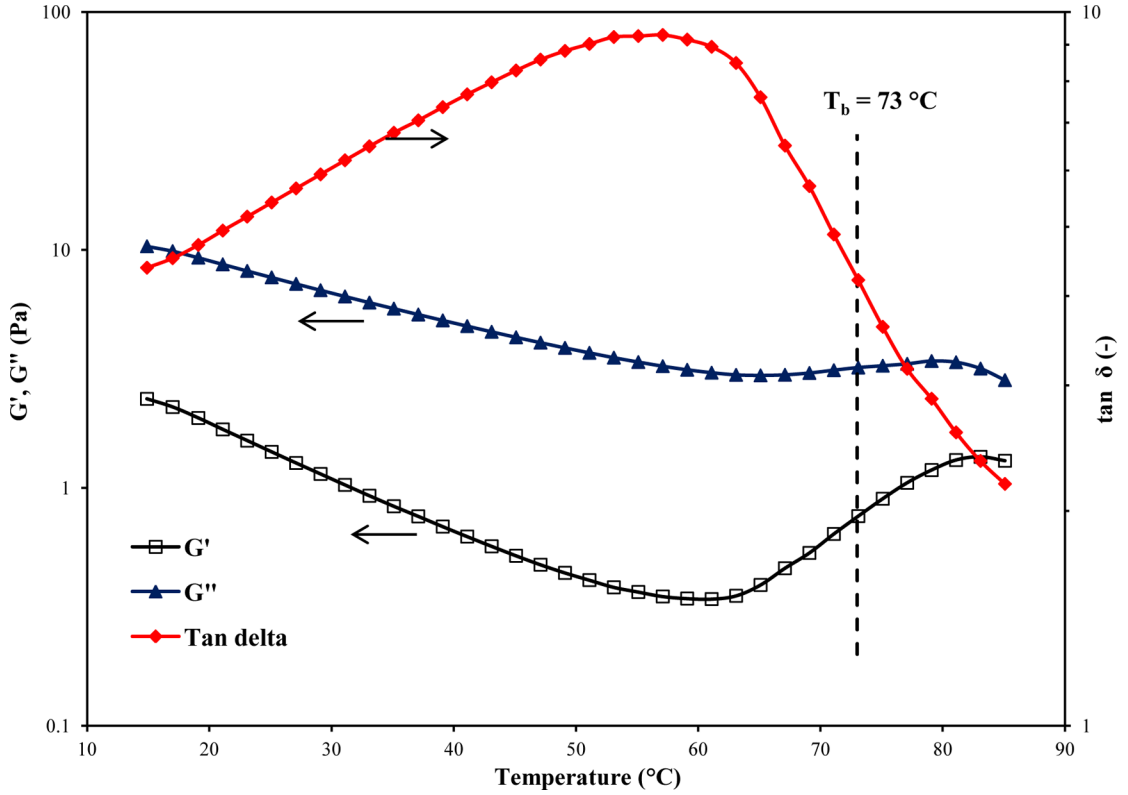

Figure 1. Isochronal dynamic temperature sweep of storage modulus (G'), loss modulus (G''), and tan δ for a solution of 6 wt % PEO in water. Measured at a fixed frequency of 1 rad/s, oscillatory stress of 2 Pa, and heating rate of 0.5 °C/min.

at a high value which decreases continuously by increasing the concentration. The minimum is reached and stayed constant at moderate concentrations and then increases steadily at highly concentrated solutions. Results of Venohr et al.[58] and Michalczyk et al.[59] showed that χ is constant at volume concentrations of 0.04−0.5 for a 10 kDa PEO grade. It is speculated that our solution concentration, which is 6 wt % ≈ 4.76 vol %, falls in this concentration range. Hence, the interaction parameter function, $g(T,\phi_2)$, is nearly independent of concentration, and eq 12 is applicable and leads to acceptable results.

The spinodal decomposition temperature is the boundary between unstable and metastable mixtures. Thermodynamically, at the spinodal points the following equation is satisfied at a certain temperature ($T = T_s$):[56,57]

$$\frac{\partial^2\left(\frac{\Delta G}{R}\right)}{\partial {\phi_2}^2} = 0 \tag{17}$$

At the binodal point, a homogeneous polymer solution separates into two phases. The general condition for equilibrium between two coexisting phases is that the chemical potential of each component must be the same in both phases.[55] It is shown that these conditions are satisfied when the so-called binodal points have a common tangent line, e.g. at ϕ_{2A} and ϕ_{2B}, in the plot of $\Delta G/RT$ versus ϕ_2.[55] Thus, at the binodal points (ϕ_{2A} and ϕ_{2B}) at $T = T_b$, the following equations must be satisfied:[60]

$$\left.\frac{\partial\left(\frac{\Delta G}{RT}\right)}{\partial \phi_2}\right|_A = \left.\frac{\partial\left(\frac{\Delta G}{RT}\right)}{\partial \phi_2}\right|_B \tag{18}$$

$$\left.\left(\frac{\Delta G}{RT} - \frac{\partial\left(\frac{\Delta G}{RT}\right)}{\partial \phi_2}\phi_2\right)\right|_A = \left.\left(\frac{\Delta G}{RT} - \frac{\partial\left(\frac{\Delta G}{RT}\right)}{\partial \phi_2}\phi_2\right)\right|_B \tag{19}$$

By applying first and second derivative on eq 16 and considering eq 12 for the interaction parameter, and inserting into eqs 17−19, three equations are obtained, containing three unknown parameters: A, B, and ϕ_{2B}. Hence, an estimation of the Flory−Huggins interaction function can be obtained from the simultaneous solution of these equations and from the phase separation temperatures, T_b and T_s, evaluated from rheological measurements. According to Flory−Huggins theory of polymer solutions, A and B in eq 12 represent the entropic and enthalpic contributions of the interaction function, respectively.[42,55]

3. EXPERIMENTAL SECTION

Materials. A commercial chitosan grade in the form of fine powder was supplied by Marinard Biotech (Rivière-au-Renard, QC, Canada). The weight-average molecular weight of this chitosan was measured by size exclusion chromatography with multiangle laser light scattering (SEC-MALLS) and was found to be 85 ± 5 kDa. The degree of deacetylation (DDA) (97.5%) was determined from ^{1}H NMR spectroscopy.[29] More on the characterization of this chitosan grade can be found in ref 29. PEO with a molecular weight of 600 kDa was obtained from Scientific Polymers Inc. (Ontario, NY). Reagent grade acetic acid (99.7%, Aldrich, Milwaukee, WI) and deionized Milli-Q water (conductivity at 25 °C < 18 μS cm^{-1}) were employed to prepare the aqueous solutions. All the materials were used as received.

Solutions Preparation. A solution of PEO in water was prepared at a concentration of 6 wt %. For a similar PEO grade (600−700 kDa) at a concentration of 2−2.5 wt % in water, a lower critical solution temperature of 99−105 °C has been reported.[4,6,10] In addition,

dx.doi.org/10.1021/ma301193h | Macromolecules 2012, 45, 7621−7633

aqueous solutions of chitosan and PEO in 50 wt % acetic acid were separately prepared at 4 wt % polymer concentration. For this solvent, the critical overlap concentrations (C^*) of chitosan and PEO are 0.1 and 0.2 wt %, respectively.[29] More on the determination of these concentrations can be found in ref 29. Therefore, the polymer concentrations used in this work are way above the critical overlap concentration. Solution mixing was performed at room temperature using a laboratory magnetic stirrer (Corning Inc., Boston, MA) for 18−24 h to ensure complete dissolution of the polymers and obtain homogeneous solutions. The prepared solutions were left to rest 4 h for degassing and kept in sealed containers at room temperature. Chitosan/PEO blend solutions at 20/80, 50/50, and 80/20 ratios were prepared by mixing the two solutions at a 4 wt % total polymer concentration.

Rheological Measurements. Dynamic rheological properties of the solutions were characterized using a stress-controlled rotational rheometer (AR-2000, TA Instruments, New Castle, DE) with a Couette flow geometry with bob and cup radius of 14 and 15 mm, respectively. A low-viscosity silicon oil was used to cover the surface of the sample solutions to prevent solvent evaporation during testing. The presence of the oil was shown not to impact the rheological measurements. The stability of the solutions as a function of time at 25 °C was examined in oscillatory shear tests under a low frequency of 1 rad/s and a small deformation of 0.1. The elastic and loss modulus decreased by less than 1 and 3%, respectively, in more than 1 h, demonstrating a good stability of the solutions.

Preliminary isothermal stress sweeps were carried out from 0.18 to 20 Pa at several fixed frequencies between 0.1 and 150 rad/s to determine the linear viscoelastic regime of the solutions. The effect of temperature on the viscoelastic response of the various solutions was studied by performing isochronal temperature sweep experiments. The storage and loss moduli were measured at a given frequency of 1 rad/s and a uniform rate of heating of 0.5 °C/min at a constant stress of 2 Pa. The temperature range of 25−80 °C was chosen to cover the whole region from homogeneous to phase-separated regions in the phase diagram. Isothermal oscillatory frequency sweeps in the range of 0.2−120 rad/s using stresses 0.5−2.5 Pa, hence well within the linear viscoelastic regime, were also performed.

Isothermal steady simple shear measurements were carried out on solutions by applying shear rates from 0.1 to 2000 s^{-1} over a temperature range of 25−80 °C. Possible fluid inertia effects at high shear rates were also examined by looking at values of the Reynolds number *Re*. In Couette flow geometry, this number is given by $Re = \rho\dot{\gamma}h^2/\eta$, where ρ is the density of the fluid, $\dot{\gamma}$ is the shear rate, h is the flow gap, and η is the viscosity of the solution.[61] The calculated *Re* values were of the order of 10^{-4}−1 over the range of shear rates used in these tests; hence, the flow conditions were considered inertialess. The zero shear viscosity of the solutions was evaluated by using the Carreau−Yasuda[62] model to the shear viscosity data when applicable.

4. RESULTS AND DISCUSSION

4.1. Determination of Solution Critical Points by Oscillatory Shear Measurements. *PEO/Water Solution.* To assess the viability of using the rheological measurements to find out the thermodynamic phase separation data of the polymer solutions, a dynamic temperature sweep test was carried out on a 6 wt % PEO solution in water. This solution was chosen since the phase behavior of PEO solutions in water has been widely reported in the literature.[1,3−9]Additionally, PEO at this content is concentrated enough to develop large torques during the rheological tests, which helps to improve the reliability of the data. Figure 1 shows the storage and loss moduli and tan δ as functions of temperature for a 6 wt % PEO/water solution at a fixed frequency of 1 rad/s and a stress of 2 Pa. The temperature was increased from 15 to 90 °C at a rate of 0.5 °C/min. The frequency of 1 rad/s was selected to make sure that the changes observed in the viscoelastic properties were only induced by phase separation rather than any other factors. Ajji et al.[52] showed that this frequency is small enough for this purpose. Figure 1 depicts that G' and G''decreases gradually with increasing temperature, which is due to the increase of PEO chain's mobility and lower intermolecular friction.[44,51,52] As temperature further increases, the storage modulus (G') increases considerably in the temperature range of 60−85 °C, and an obvious upturn appears. A modest increase in the loss modulus is also observed. On the other hand, tan δ shows a reverse trend: a gradual increase followed by a sudden reduction with increasing temperature. Based on the known LCST behavior of PEO/water solutions, phase separation occurs in this temperature range. In the vicinity of phase separation, the thermodynamic forces emerge as a competing phenomenon to chain mobility. By approaching the solution segregation temperature, these forces dominate and control the viscoelastic behavior of the solution. It is believed that the temperature range in which the viscoelastic behavior is more influenced by the thermodynamic forces is related to the phase separation region.[45,46,50] For temperatures higher than this temperature range, mobility forces control again the viscoelastic behavior of the resulted phase-separated blend, and thus, storage and loss modulus decrease again.[47]

The observed remarkable increase of the elasticity during the dynamic temperature sweep is most probably related to the morphology changes and domain growth that occur during the phase separation of the solution. This elasticity enhancement originates mainly from two sources: concentration fluctuations resulting from chain mobility and thermodynamic forces[45,46,52] and formation of new interfaces during phase separation that brings in additional elasticity to the system.[43] PEO-rich domains may form during the segregation process, and the deformation and shape recovery of these domains may enhance the elasticity. This phenomenon can be considered as interfacial tension-driven elasticity, as seen in molten polymer blends.[44] Therefore, it is predictable that the storage modulus, G', and loss tangent, tan δ, would be more sensitive to temperature changes since the stress induced to the system by the concentration fluctuations and the new interface formation have mostly an elastic origin that affect more the elastic modulus. The developed equations for G' and G'' (eqs 6 and 7 in section 2) by Ajji and Choplin[48] also confirm this dependency.

Figure 1 can be used to determine the binodal decomposition temperatures or cloud points. The temperature at the inflection point of G' or tan δ versus temperature, i.e., the temperature at the minimum dG'/dT, is assigned as the binodal temperature.[44,45,63] For the 6 wt % PEO water solution, a binodal temperature of 73 °C is obtained by this method, indicated by the dashed line in Figure 1. The reported cloud point in the literature for PEO with similar molecular weight is around 85−90 °C.[4,6,10] The discrepancy between the binodal points obtained from rheometry with that measured by light scattering could be attributed to the aforementioned[7,13] clustering effect in aqueous PEO solutions.

Formation of clusters at temperatures well below the phase separation temperature of PEO solution in water was investigated by several researchers using light and neutron scattering methods.[2,5,7,9,13,64] They showed that undissolvable aggregates increased when the PEO solution was heated to temperatures higher than 30 °C. They found that clusters concentration dramatically increased when the temperature was still 30 °C below the cloud point of the solution. A cluster size

dx.doi.org/10.1021/ma301193h | Macromolecules 2012, 45, 7621−7633

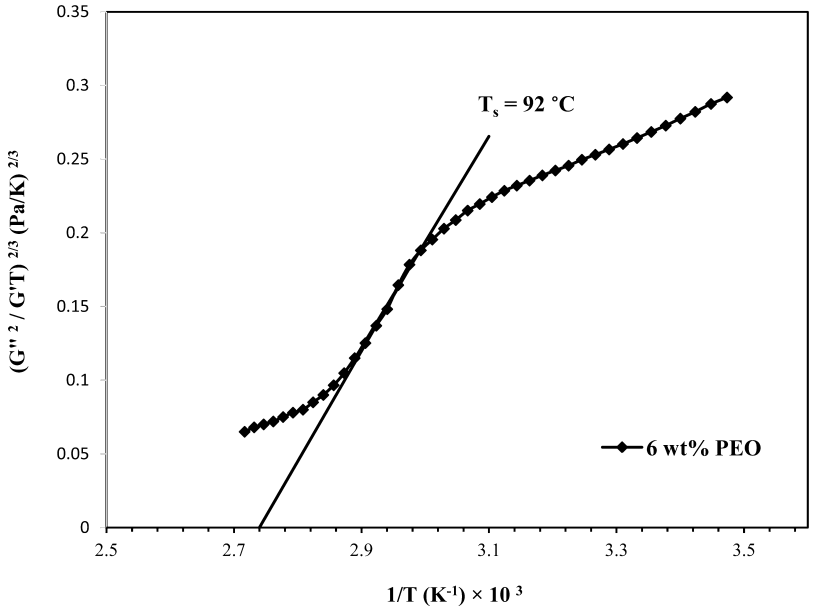

Figure 2. Estimation of spinodal temperature from the quantitative evaluation of the viscoelastic behavior of a 6 wt % PEO in water near the phase boundary (data is from Figure 1). The spinodal temperature is indicated in the figure by the intercept of the curve in the linear region.

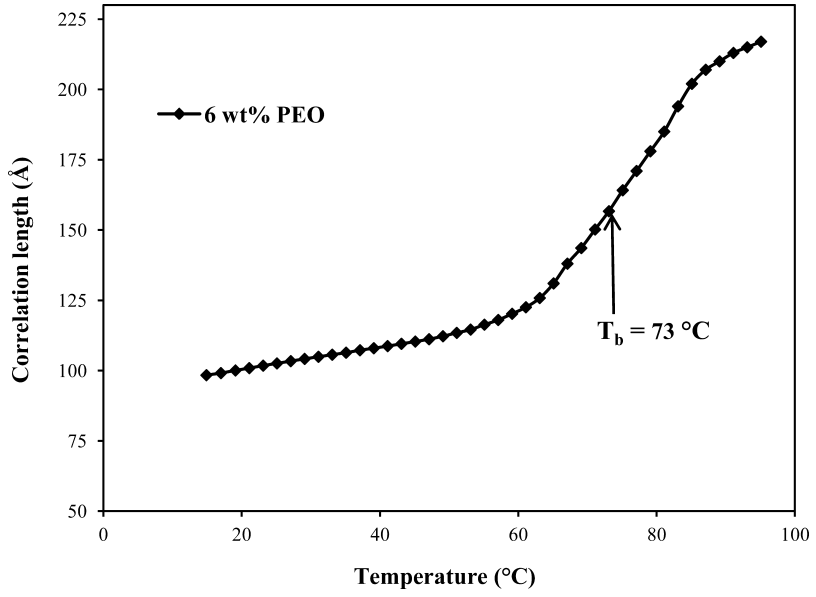

Figure 3. Temperature dependence of the correlation length, ξ for the 6 wt % PEO solution in water obtained quantitatively from eq 11 (section 2) and isochronous dynamic temperature sweep data (Figure 1).

of 1.36 μm for a 4 wt % solution of 100 kDa PEO, and 740 nm for a very dilute (20 ppm) solution of 1000 kDa PEO in water, has been reported in the literature.[3,7] Clustering has been ignored in all proposed thermodynamic models for predicting PEO/water phase diagram and the phase separation behavior.[1,7,9] Only de Gennes[65] attempted to explain the clustering effect in aqueous PEO solutions by considering a novel second type of phase separation occurring well below the conventional LCST point, in which a very dilute solution of collapsed coils coexists with a dense polymer phase (i.e., clusters or aggregates).[9] It is speculated that the binodal temperature measured by rheological measurements in Figure 1 is somehow associated with this phase separation phenomenon, as it is 10–20 °C below the reported cloud point for this sample and hence in good agreement with cluster formation temperatures reported in the literature.[5,9,65] The anomalous rheological behavior of dilute PEO solutions was also ascribed to the presence of aggregates (or clusters) in PEO solutions.[3] PEO clusters coexist in equilibrium with free polymer coils is solution.[3,5] These clusters are mainly formed from high-molecular-weight spherulites and low-density noncrystalline microgels[2,3,5] and can both induce significant elasticity to the system.[3]

The spinodal decomposition temperature of the solution can be estimated by applying the quantitative Ajji and Choplin's[48] modified approach of Frederickson and Larson[49] theory (section 2).

Figure 2 displays $(G''^2/G'T)^{2/3}$ versus $1/T$ for the 6 wt % PEO solution in water. As mentioned in section 2, the linear region in Figure 2 corresponds to the one-phase region near the

dx.doi.org/10.1021/ma301193h | *Macromolecules* 2012, 45, 7621–7633

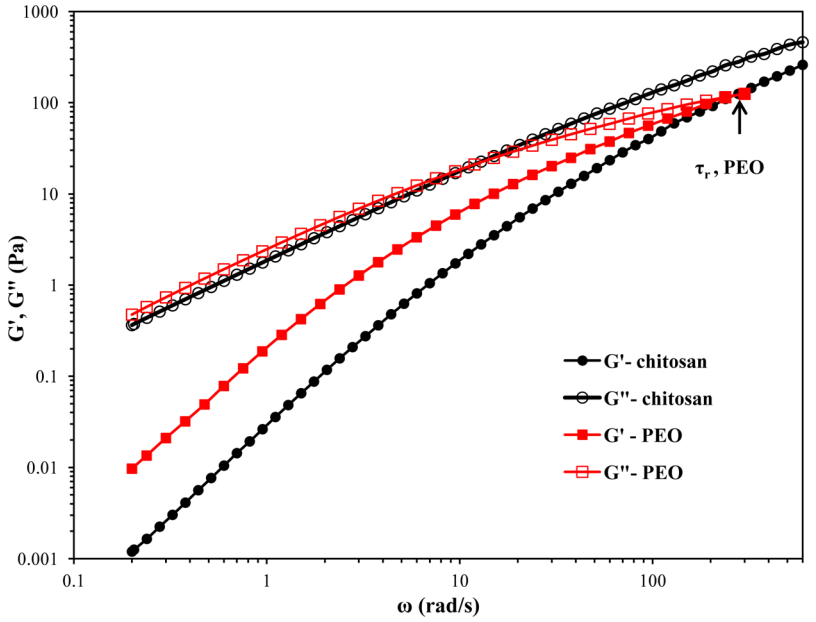

Figure 4. Frequency sweep plots of storage modulus, G', and loss modulus, G'', for 4 wt % solutions of neat chitosan and PEO in 50 wt % aqueous acetic acid at 25 °C.

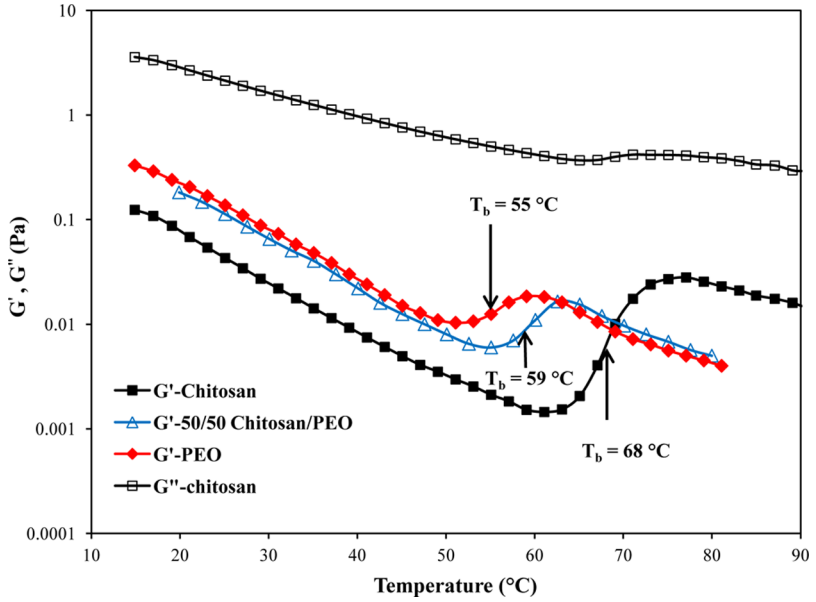

Figure 5. Isochronal dynamic temperature sweep of storage modulus (G') and loss modulus (G'') for 4 wt % solutions of chitosan, PEO, and their 50/50 blend in 50 wt % aqueous acetic acid solution. Measured at a fixed frequency of 1 rad/s, oscillatory stress of 2 Pa, and heating rate of 0.5 °C/min. Vertical lines show the rheologically determined binodal temperatures at the inflection points of G' vs temperature curves.

phase separation point. In this curve, the reciprocal of the intercept with the $1/T$ axis is assumed to be the spinodal temperature, T_s, that was calculated to be about 92 ± 3 °C for the PEO solution in Figure 2. The error associated with the evaluation of the spinodal temperature is approximately ±3 °C, based on the selection of the fitted line on the linear region of the curve. The obtained spinodal temperature by this method agrees well with the T_s points obtained by Hammouda and co-workers from SANS measurements. They reported spinodal temperatures of 105 and 95 °C for 4 wt % solutions of 50 and 100 kDa PEO in water, respectively.[7,13]

Figure 3 shows the changes in the correlation length, ξ of the PEO solution with temperature near the phase separation region. The data plotted in this figure were determined from eq 11 (section 2), by using the rheological data of Figure 1. The correlation length is related to concentration fluctuations. Significant changes in correlation length in the phase separation area represent the changes of the degree of local ordering and increased composition fluctuations during phase separation.[44] The order of magnitude of the correlation length obtained in this work through rheological measurements is almost the same as that reported by Hammouda et al.[13] obtained by the SANS method. They found correlation length of 40−400 Å for a 4 wt % solution of 100 kDa PEO in water.[13] This also validates again the rheological technique to find out thermodynamic properties. The binodal temperature is indicated in Figure 3, and it is

dx.doi.org/10.1021/ma301193h | Macromolecules 2012, 45, 7621−7633

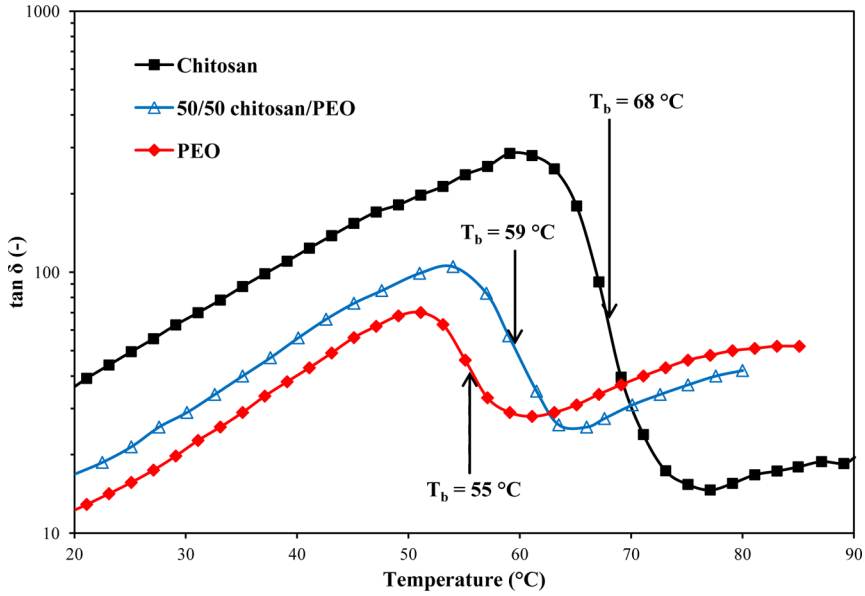

Figure 6. Isochronal dynamic temperature sweep of loss tangent angle (tan δ) for 4 wt % neat chitosan, PEO, and their 50/50 blend in 50 wt % aqueous acetic acid solution. Measured at a fixed frequency of 1 rad/s, oscillatory stress of 2 Pa, and heating rate of 0.5 °C/min. Vertical lines show the rheologically determined binodal temperatures at the inflection points of tan δ vs temperature curves.

indeed located in the transition range, close to the inflection point.

Chitosan/PEO Aqueous Acetic Acid Solutions. After showing that rheological measurements can be employed successfully to determine the phase separation behavior of a polymer solution, the same procedure is used for the solutions of interest here, i.e., chitosan, PEO, and their blends in aqueous acidic solutions. As mentioned before, these solutions have shown anomalous behavior during fiber electrospinning at elevated temperatures,[29] which was suspected to be due to phase separation during the process.

Dynamic rheological properties of the neat solutions of chitosan and PEO in aqueous acetic acid were measured by isothermal frequency sweep experiments at 25 °C. The results are shown in Figure 4. This figure depicts that the elastic modulus of PEO is higher than that of chitosan up to a frequency of 300 rad/s. The characteristic relaxation time, τ_r, obtained from the reciprocal of the frequency where $G' = G''$(~5 ms) is longer for PEO than chitosan. In fact, this intersection point for chitosan falls outside the frequency range studied in this work and hence is shorter than ~1 ms. The characteristic relaxation time of the polymer chains is related to the monomeric friction coefficient or chain entanglements.[66] Lower elasticity and shorter relaxation time for chitosan are probably due to repulsive forces between NH_3^+ groups formed in acidic media. This may reduce chain entanglements and result in a rigid rod-like chain conformation in the solution state.[15,18]

To elucidate the phase behavior of aqueous acetic acid solutions of chitosan and PEO with temperature, the method used above for PEO/water solution was applied. Dynamic isochronal temperature sweep tests were carried out on the neat chitosan and PEO solutions and their blends at different composition ratios of 80/20, 50/50, and 20/80.

Figures 5 and 6 present the evolution of the storage modulus (G') and tan δ, respectively, during dynamic temperature sweeps at a fixed frequency of 1 rad/s and oscillatory stress of 2 Pa for 4 wt % chitosan, PEO, and their 50/50 blend solutions. Again, the temperature was increased from 15 to 90 °C at a rate of 0.5 °C/min. Similar behaviors to that observed previously for the PEO/water solution (Figure 1) can be depicted in Figures 5 and 6, i.e., a gradual decrease of G' with temperature along with a clear upturn at higher temperatures and a reverse trend for the tan δ curves. Therefore, it can be concluded that all these solutions also exhibit an LCST in their phase diagram, as they reveal phase separation behavior with increasing temperature. This is attributed to the presence of specific interactions due to hydrogen bonds formed between hydroxyl groups of acetic acid/water solvent and ether groups in PEO and hydroxyl and amino groups in chitosan.[14,16,29] It is well-known that solutions with strong solvent/polymer interactions show an LCST phase diagram.[1,3,8] The binodal temperature, T_b, of PEO in 50 wt % acetic acid solvent is evaluated to be 55 °C from Figures 5 and 6, quite different from the value of 73 °C determined in Figure 1 for the binodal temperature of PEO in water. This is probably due to the different solubility of PEO in acetic acid and water, resulting from different strength of interaction between PEO chains and acetic acid as compared to that with water molecules. This difference also leads to different expansion behavior of the PEO chains in these two solutions.[29]

It is interesting to note that, over the tested temperature range, the 50/50 blend solution exhibits a single peak located between the peaks of its neat polymer constituents. This indicates full miscibility of chitosan and PEO in the solution state; hence, a homogeneous solution up to phase separation temperatures. Additionally, it is also apparent from Figures 5 and 6 that not only the magnitude of the upturn and reduction of the storage modulus and loss tangent angle, respectively, strongly depend on solution composition but also the temperature range over which the sharp changes occur. The binodal decomposition temperatures, T_b, of the solutions were estimated using the same approach as for the PEO/water solution (Figure 1). Inflection points of G' and tan δ curves versus temperature gave estimates of binodal temperatures of about 68, 55, and 59 °C for neat chitosan, neat PEO, and their 50/50 blend solutions, respectively. These points are indicated

dx.doi.org/10.1021/ma301193h | *Macromolecules* 2012, 45, 7621−7633

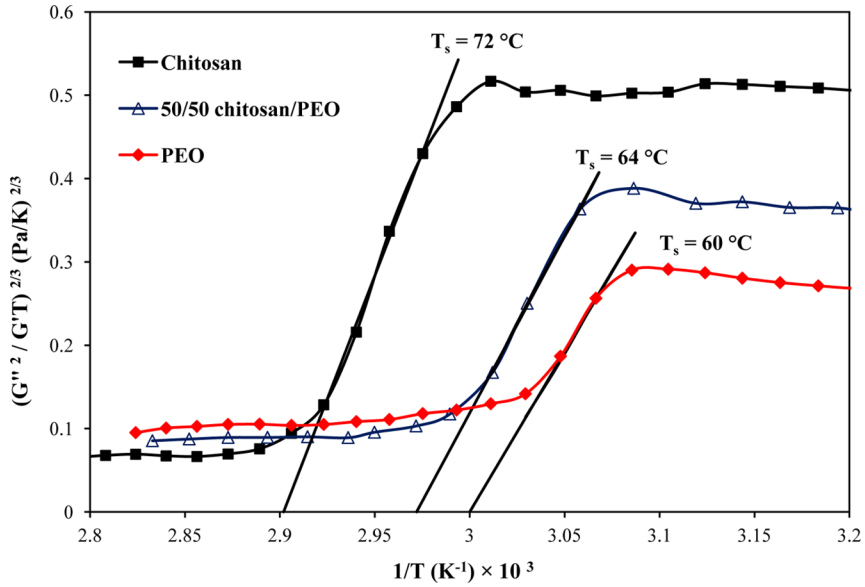

Figure 7. Estimation of spinodal temperature from the quantitative evaluation of the viscoelastic behavior of neat chitosan, PEO, and their 50/50 blend in 50 wt % aqueous acetic acid, near the phase boundary (data are from Figure 5). The spinodal temperatures are indicated in the figure from the intercept of the curves in the linear region.

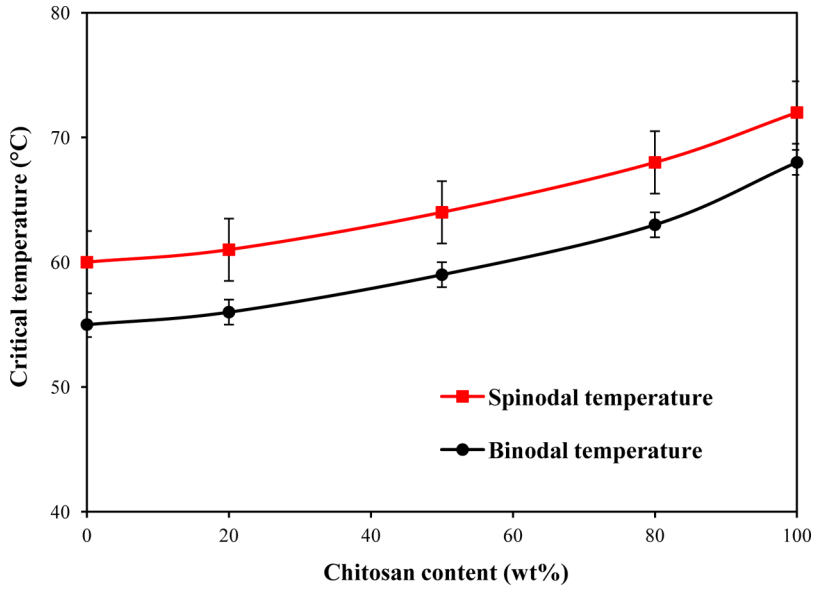

Figure 8. Binodal and spinodal phase separation temperatures of neat chitosan, neat PEO, and their blends at different ratios in 50 wt % aqueous acetic acid (total polymer concentration is 4 wt % for all solutions).

by arrows in Figures 5 and 6. The evaluations from G' and tan δ resulted in the same value of T_b for each composition. Similar results were obtained for the 20/80 and 80/20 solutions, but the corresponding curves are not shown for the sake of clarity. The binodal and spinodal temperatures evaluated for these two blends are reported in Figure 8.

The approach taken in Figure 2 was also employed to quantitatively evaluate the spinodal decomposition temperatures of PEO/chitosan solutions. Figure.7 presents $(G''^2/G'T)^{2/3}$ versus $1/T$ for the 4 wt % solutions of neat PEO, neat chitosan solution, and their 50/50 blend in 50 wt % aqueous acetic acid solution. Spinodal temperatures, T_s, were determined to be 72, 60, and 64 °C for neat chitosan, neat PEO, and their 50/50 blend solutions, respectively. An error of about ±2.5 °C is involved in these values.

Binodal and spinodal decomposition temperatures of aqueous acetic acid solutions of chitosan and PEO and their blends, determined by temperature sweep experiments, are shown in Figure 8 as functions of chitosan content. It depicts that, for the same 4 wt % total polymer concentration, chitosan has the higher LCST temperature. It means that chitosan in the aqueous acetic acid solvent has a larger one-phase homogeneous region as compared to PEO. It is known that LCST phase behavior in polymer solutions is typical of systems that exhibit hydrogen bonds. Hydrogen bond weakening or complete debonding occurs with a temperature increase.[1,8,9] Higher LCST in chitosan could be due to more intense interactions with the acetic acid/water solvent. While PEO can form hydrogen bonds only via its ether groups, chitosan has more active groups such as hydroxyl, acetylamine, and amino

dx.doi.org/10.1021/ma301193h | *Macromolecules* 2012, 45, 7621−7633

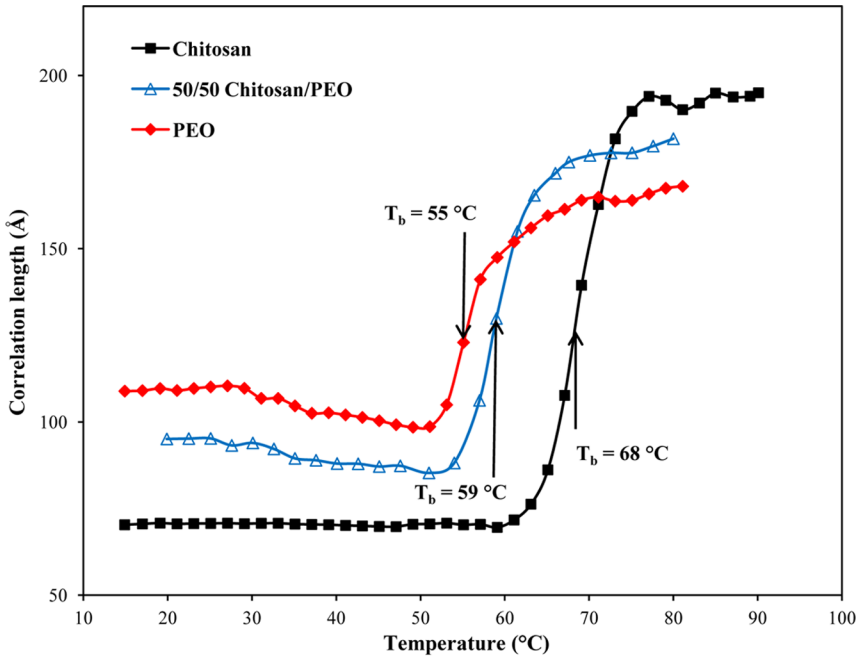

Figure 9. Temperature dependence of the correlation length, ξ, for neat chitosan, neat PEO, and their 50/50 blend in 50 wt % aqueous acetic acid obtained quantitatively from the rheological measurements.

groups to form hydrogen bonds.[14,19] Therefore, temperature-induced disruption in polymer/solvent interactions affects more PEO and leads to an earlier phase separation lower critical temperature. Binodal and spinodal decomposition temperatures of chitosan/PEO blends are located between those of neat chitosan and PEO solutions, which is again an indication of their miscibility in the solution state prior to phase separation.

It is worth noting that both estimated binodal and spinodal temperatures for PEO in aqueous acetic acid solvent are about 15−20 °C lower than for PEO in water (Figures 2 and 3). It indicates that the degree of association between PEO and the solvent in aqueous acetic acid solution is reduced earlier by increasing temperature. This is more likely due to weaker or fewer hydrogen bonds formed between acetic acid and PEO, as compared to PEO and water molecules. In PEO/water solution it is suggested that two water molecules are associated with each PEO monomer, that at the same time are in competition to form water−water hydrogen bonds with their neighboring water molecules.[1,8] These prevailing hydrogen bonds are responsible for the unusual aforementioned characteristics of PEO solutions in water.

Plots of the correlation length (ξ) evaluated from eq 11 (section 2) as a function of temperature in the vicinity of phase separation for neat chitosan, PEO, and their 50/50 blend are shown in Figure 9. The orders of magnitude of the correlation length of these solutions and PEO solution in water (Figure 3) are almost the same. It reflects that concentration fluctuations and the process of phase separation in these polymer solutions are similar. Binodal decomposition temperatures are also indicated in Figure 9 and are located in the transition range, close to the inflection point.

4.2. Isothermal Steady Shear Viscosity Results. Steady shear viscosity as a function of shear rate and temperature for solutions of 4 wt % neat chitosan and its 50/50 blend with 4 wt % PEO in 50 wt % aqueous acetic acid is shown in Figure 10. The experiments were carried out from 25 to 70−80 °C over a shear rate range of 0.1−1000 s^{-1}. A typical shear-thinning behavior with a well-developed plateau region is observed for neat chitosan solutions up to 60 °C (Figure 10A). This figure also shows that the magnitude of the zero-shear viscosity decreases with an increase of temperature up to 60 °C and that the critical shear rate for the onset of shear-thinning increases as the temperature is raised. However, at a temperature of 70 °C, an enhancement in the viscosity is observed at low shear rates (Figure 10A). This temperature is near the phase separation point of this solution that was estimated to have a binodal temperature of 68 °C (section 4.1). This enhancement in viscosity at low shear rates may be explained by Onuki's[67] interpretation of the viscosity of a phase separating two-component fluid near the critical point and its similarity with a suspension of droplets in a fluid after the formation of sharp interfaces and phase-separated domains near the critical point.[67] The same behavior is also observed for the 50/50 blend of chitosan/PEO in aqueous acetic acid solution (Figure 10B). In this solution, the increase of viscosity at low shear rates is detected at temperatures as low as 60 °C, which is in agreement with its determined binodal phase separation temperature (59 °C). These results are in contrast with Sharma's[50] findings for a polymer blend system, who reported that the overall behavior of viscosity versus shear rate remains unchanged at temperatures before and after the phase separation point. This is possibly because Sharma tried to apply the Onuki's approach, developed for polymer solutions, to a molten polymer blend that may not have emulsion-type morphology.

4-3. Flory−Huggins Interaction Parameter from Rheological Data. The temperature dependence of the Flory−Huggins interaction parameter, χ, of the solutions investigated was evaluated from the basic thermodynamic approach described in section 2.2 and the binodal and spinodal points estimated from rheological measurements (section 4.1). The computed A and B coefficients (eq 12) and interaction parameter at certain temperatures are reported in Table 1. Absolute values of χ at given temperatures and the related coefficients, A and B, in the case of the PEO/water solution,

dx.doi.org/10.1021/ma301193h | Macromolecules 2012, 45, 7621−7633

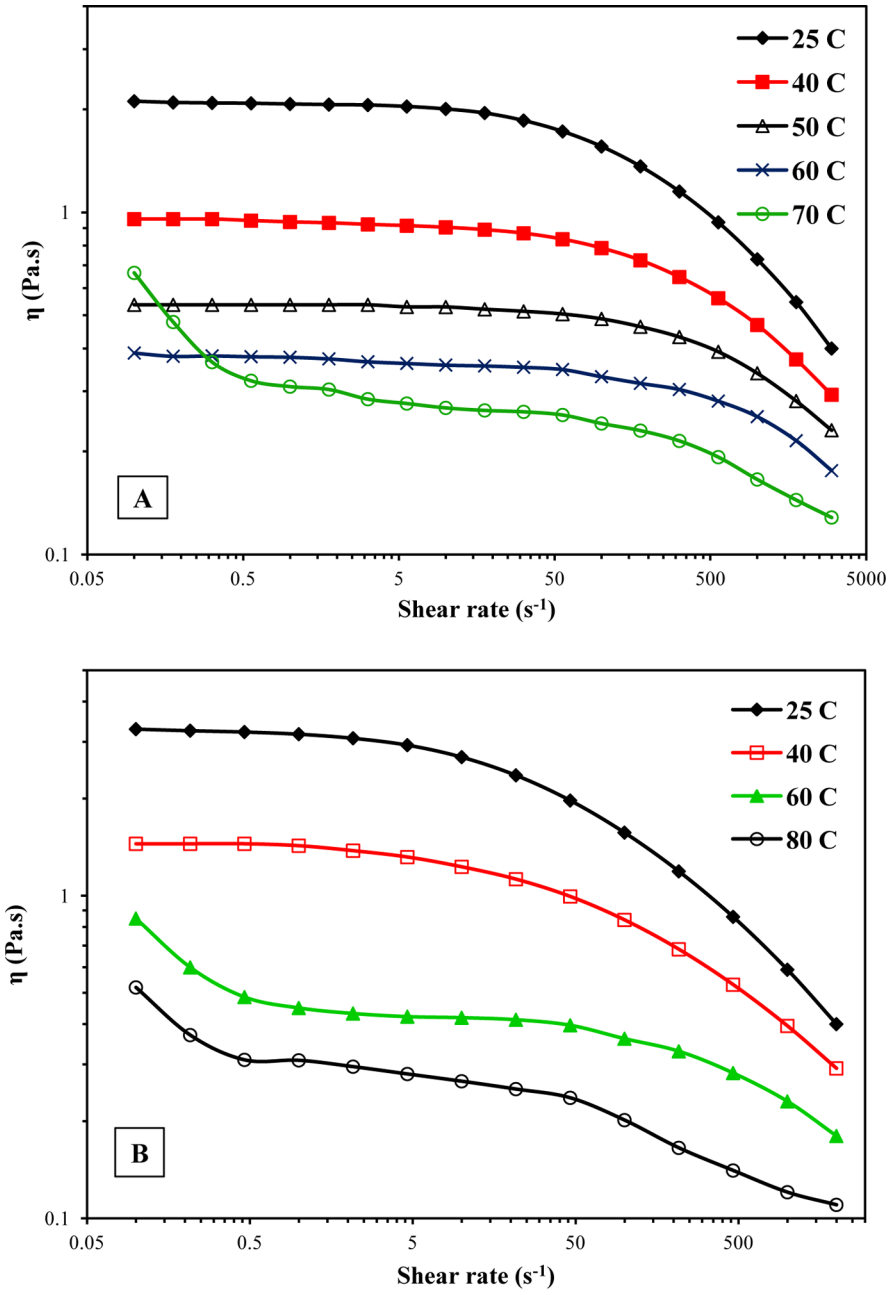

Figure 10. Plot of isothermal shear viscosity versus shear rate for (A) 4 wt % neat chitosan solution and (B) its 50/50 blend with 4 wt % PEO over the temperature range covering homogeneous to the two-phase regimes of the solutions phase behaviors, all in 50 wt % aqueous acetic acid solvent.

Table 1. *A* and *B* Coefficients of Flory–Huggins Interaction Parameter, Eq 12, and Values of the Interaction Parameter, χ, at Given Temperatures Obtained by Using Different Experimental Methods

reference	method	solvent	polymer	*A*	*B*	*T* (°C)	interaction parameter (χ)
this paper	rheometry	water	PEO, 600 kDa	0.8	−100	25	0.4644
Venohr et al.[58]	dynamic and static light scattering	water	PEO, 20 kDa	0.8	−108		
Venohr et al.[58]	dynamic and static light scattering	water	PEO, 100 kDa			20	0.4653
Polik and Borchard[5]	static light scattering	water	PEO, 17 kDa	0.51	−3	25	0.5
Michalczyk and Borchard[59]	vapor pressure osmometry	water	PEO, 100 kDa	0.66	−71		
Fischer[37]	turbidity observation	water	PEO, 6 kDa	2.41	−730.5		
Bae et al.[56]	vapor sorption	water	PEO, 8 kDa			30	0.349
Safranov and Zubarev[68]	calculation of enthalpy of dilution	0.3 M acetic acid	chitosan, 88% DDA			25	−0.01
this work	rheometry	50 wt % acetic acid	PEO, 600 kDa	0.85	−120	25	0.4404
this work	rheometry	50 wt % acetic acid	chitosan, 98% DDA	0.9	−150	25	0.388

dx.doi.org/10.1021/ma301193h | *Macromolecules* 2012, 45, 7621−7633

coincide well with results reported in the literature obtained by light scattering, gas chromatography, and vapor pressure osmometry techniques. The negative value of B confirms the existence of LCST phase diagrams in the PEO/chitosan solutions.

5. CONCLUSIONS

In this work a systematic rheological investigation of the well-known LCST polymer solution of PEO in water was conducted. We showed that the phase separation temperature of this solution could be assessed directly by rheological measurements. Binodal points were estimated from dynamic temperature sweep experiments, and spinodal points were quantitatively calculated on the basis of a mean-field theory. Comparing these critical points with that obtained from other experimental techniques showed that rheological measurements can sensitively detect rather early stages of phase separation.

This approach was then employed on our solutions of interest: chitosan/PEO at different ratios in aqueous acetic acid. These solutions showed a LCST phase diagram as well, originating mainly from the existence of hydrogen bonds. Knowledge of phase separation temperature of chitosan-based solutions is crucial for chitosan wet route formation processes. Additionally, occurrence of a viscosity enhancement in isothermal steady shear measurements right after phase separation confirms the validity of the aforementioned approach to determine solution critical points. The Flory–Huggins interaction parameter was calculated from the binodal and spinodal points estimated by the rheological measurements. The obtained results agreed well with reported data in the literature for aqueous PEO solution which validate further the rheometry-based approach used in this work. Additionally, this parameter was estimated for the first time for chitosan solutions in 50 wt % aqueous solution. Therefore, rheology provides a powerful and simple technique to assess the phase separation behavior of polymer solutions.

■ AUTHOR INFORMATION

Corresponding Author

*Ph 01-514 340 4711 ext 5390, e-mail marie-claude.heuzey@polymtl.ca (M.-C.H.); Ph 01-514 340 4711, e-mail abdellah.ajji@polymtl.ca (A.A.).

Notes

The authors declare no competing financial interest.

■ ACKNOWLEDGMENTS

The authors acknowledge the financial support of this work by NSERC (National Science and Engineering Research Council of Canada) and FRQNT (Fonds de recherche du Québec - Nature et technologies).

■ REFERENCES

(1) Dormidontova, E. E. *Macromolecules* **2002**, *35* (3), 987–1001.
(2) Duval, M.; Sarazin, D. *Polymer* **2000**, *41* (7), 2711–2716.
(3) Shetty, A. M.; Solomon, M. J. *Polymer* **2009**, *50* (1), 261–270.
(4) Saeki, A.; Kuwahara, N.; Nakata, M.; Kaneko, M. *Macromolecules* **1976**, *17*, 685–689.
(5) Polic, W. F.; Burchard, W. *Macromolecules* **1983**, *16*, 978–982.
(6) Bae, Y. C.; Lambert, S. M.; Soane, D. S.; Prausnitz, J. M. *Macromolecules* **1991**, *24* (15), 4403–4407.
(7) Hammouda, B.; Ho, D. L.; Kline, S. *Macromolecules* **2004**, *37* (18), 6932–6937.
(8) Dormidontova, E. E. *Macromolecules* **2004**, *37* (20), 7747–7761.
(9) Bekiranov, S.; Bruinsma, R.; Pincus, P. *Phys. Rev. E* **1997**, *55* (1), 577–585.
(10) Fischer, V.; Borchard, W. *J. Phys. Chem. B* **2000**, *104* (18), 4463–4470.
(11) Esquenet, C.; Buhler, E. *Macromolecules* **2002**, *35* (9), 3708–3716.
(12) Esquenet, C.; Buhler, E. *Macromolecules* **2001**, *34* (15), 5287–5294.
(13) Hammouda, B.; Ho, D.; Kline, S. *Macromolecules* **2002**, *35* (22), 8578–8585.
(14) Rinaudo, M. *Prog. Polym. Sci.* **2006**, *31* (7), 603–632.
(15) Pillai, C. K. S.; Paul, W.; Sharma, C. P. *Prog. Polym. Sci.* **2009**, *34* (7), 641–678.
(16) Schatz, C.; Viton, C.; Delair, T.; Pichot, C.; Domard, A. *Biomacromolecules* **2003**, *4* (3), 641–648.
(17) Kumar, M. *React. Funct. Polym.* **2000**, *46* (1), 1–27.
(18) Kumar, M.; Muzzarelli, R. A. A.; Muzzarelli, C.; Sashiwa, H.; Domb, A. J. *Chem. Rev.* **2004**, *104* (12), 6017–6084.
(19) Philippova, O. E.; Volkov, E. V.; Sitnikova, N. L.; Khokhlov, A. R.; Desbrieres, J.; Rinaudo, M. *Biomacromolecules* **2001**, *2* (2), 483–490.
(20) Dash, M.; Chiellini, F.; Ottenbrite, R. M.; Chiellini, E. *Prog. Polym. Sci.* **2011**, *36* (8), 981–1014.
(21) Riva, R.; Ragelle, H.; des Rieux, A.; Duhem, N.; Jerome, C.; Preat, V. *Adv. Polym. Sci.* **2011**, *244*, 19–44.
(22) Jayakumar, R.; Menon, D.; Manzoor, K.; Nair, S. V.; Tamura, H. *Carbohydr. Polym.* **2010**, *82* (2), 227–232.
(23) Dutta, P. K.; Tripathi, S.; Mehrotra, G. K.; Dutta, J. *Food Chem.* **2009**, *114* (4), 1173–1182.
(24) Jayakumar, R.; Prabaharan, M.; Nair, S. V.; Tamura, H. *Biotechnol. Adv.* **2010**, *28* (1), 142–150.
(25) Correlo, V. M.; Boesel, L. F.; Bhattacharya, M.; Mano, J. F.; Neves, N. M.; Reis, R. L. *Mater. Sci. Eng., A* **2005**, *403* (1–2), 57–68.
(26) Epure, V.; Griffon, M.; Pollet, E.; Averous, L. *Carbohydr. Polym.* **2011**, *83* (2), 947–952.
(27) Mir, S.; Yasin, T.; Halley, P. J.; Siddiqi, H. M.; Nicholson, T. *Carbohydr. Polym.* **2011**, *83* (2), 414–421.
(28) Zivanovic, S.; Li, J. J.; Davidson, P. M.; Kit, K. *Biomacromolecules* **2007**, *8* (5), 1505–1510.
(29) Pakravan, M.; Heuzey, M. C.; Ajji, A. *Polymer* **2011**, *52*, 4813–4824.
(30) Kuo, Y. C.; Ku, I. N. *Biomacromolecules* **2008**, *9* (10), 2662–2669.
(31) Mucha, M.; Piekielna, J.; Wieczorek, A. *Macromol. Symp.* **1999**, *144*, 391–412.
(32) Islam, A.; Yasin, T. *Carbohydr. Polym.* **2012**, *88* (3), 1055–1060.
(33) Chuang, W. Y.; Young, T. H.; Yao, C. H.; Chiu, W. Y. *Biomaterials* **1999**, *20* (16), 1479–1487.
(34) Sarasam, A.; Madihally, S. V. *Biomaterials* **2005**, *26* (27), 5500–5508.
(35) Sarasam, A. R.; Krishnaswamy, R. K.; Madihally, S. V. *Biomacromolecules* **2006**, *7* (4), 1131–1138.
(36) Sionkowska, A. *Prog. Polym. Sci.* **2011**, *36* (9), 1254–1276.
(37) Fischer, V.; Borchard, W.; Karas, M. *J. Phys. Chem.* **1996**, *100* (39), 15992–15999.
(38) Ataman, M. *Colloid Polym. Sci.* **1987**, *265*, 19–25.
(39) He, M. J.; Liu, Y. M.; Yi, F.; Ming, J.; Han, C. C. *Macromolecules* **1991**, *24* (2), 464–473.
(40) Lal, J.; Bansil, R. *Macromolecules* **1991**, *24* (1), 290–297.
(41) Koningsveld, R.; Kleintjens, L. A. *Macromolecules* **1971**, *4* (5), 637–641.
(42) Flory, P. J. *Principles of Polymer Chemistry*; Cornell University Press: Ithaca, NY, 1953.
(43) Bousmina, M.; Lavoie, A.; Riedl, B. *Macromolecules* **2002**, *35* (16), 6274–6283.
(44) Niu, Y. H.; Wang, Z. G. *Macromolecules* **2006**, *39* (12), 4175–4183.

(45) Kapnistos, M.; Hinrichs, A.; Vlassopoulos, D.; Anastasiadis, S. H.; Stammer, A.; Wolf, B. A. *Macromolecules* **1996**, *29* (22), 7155−7163.
(46) Vlassopoulos, D.; Koumoutsakos, A.; Anastasiadis, S. H.; Hatzikiriakos, S. G.; Englezos, P. *J. Rheol.* **1997**, *41* (3), 739−755.
(47) Yeganeh, J. K.; Goharpey, F.; Foudazi, R. *Macromolecules* **2010**, *43* (20), 8670−8685.
(48) Ajji, A.; Choplin, L. *Macromolecules* **1991**, *24* (18), 5221−5223.
(49) Fredrickson, G. H.; Larson, R. G. *J. Chem. Phys.* **1987**, *86* (3), 1553−1560.
(50) Sharma, J.; Clarke, N. *J. Phys. Chem. B* **2004**, *108* (35), 13220−13230.
(51) Gharachorlou, A.; Goharpey, F. *Macromolecules* **2008**, *41* (9), 3276−3283.
(52) Ajji, A.; Choplin, L.; Prudhomme, R. E. *J. Polym. Sci., Part B: Polym. Phys.* **1991**, *29*, 1573−1578.
(53) Madbouly, S. A.; Ougizawa, T. *Macromol. Chem. Phys.* **2004**, *205* (9), 1222−1230.
(54) Ajji, A.; Choplin, L.; Prudhomme, R. E. *J. Polym. Sci., Part B: Polym. Phys.* **1988**, *26*, 2279−2289.
(55) Gedde, U. W. *Polymer Physics*; Chapman & Hall: London, 1995.
(56) Bae, Y. C.; Shim, J. J.; Soane, D. S.; Prausnitz, J. M. *J. Appl. Polym. Sci.* **1993**, *47* (7), 1193−1206.
(57) Qian, C. B.; Mumby, S. J.; Eichinger, B. E. *Macromolecules* **1991**, *24* (7), 1655−1661.
(58) Venohr, H.; Fraaije, V.; Strunk, H.; Borchard, W. *Eur. Polym. J.* **1998**, *34* (5−6), 723−732.
(59) Michalczyk, A.; Borchard, W. *Eur. Polym. J.* **1989**, *25* (9), 957−959.
(60) Kim, S. S.; Lloyd, D. R. *Polymer* **1992**, *33* (5), 1047−1057.
(61) Yosick, J. A.; Giacomin, J. A.; Stewart, W. E.; Ding, F. *Rheol. Acta* **1998**, *37* (4), 365−373.
(62) Carreau, P. J.; De Kee, D.; Chabra, P. R. *Rheology of Polymeric Systems: Principles and Applications*; Hanser Publishers: Munich, 1997.
(63) Patel, A. J.; Balsara, N. P. *Macromolecules* **2007**, *40* (5), 1675−1683.
(64) Pang, P.; Englezos, P. *Fluid Phase Equilib.* **2002**, *194*, 1059−1066.
(65) de Gennes, P. G. *C. R. Acad. Sci., Ser. II* **1991**, *313* (10), 1117−1122.
(66) Doi, M.; Edwards, S. F. *The Theory of Polymer Dynamics*; Oxford University Press: New York, 1986.
(67) Onuki, A. *Phys. Rev. A* **1987**, *35* (12), 5149−5155.
(68) Safronov, A. P.; Zubarev, A. Y. *Polymer* **2002**, *43* (3), 743−748.